Direct experimental evidence of multiparticle-hole ground state configuration of deformed ^{33}Mg

Ushasi Datta[1,2,*] A. Rahaman[1], T. Aumann[2,3], S. Beceiro-Novo[4], K. Boretzky[2], C. Caesar[2], B.V. Carlson[5], W.N. Catford[6], S. Chakraborty[1], M. Chartier[7], G.De. Angelis[8], D. Cortina-Gil[4], D. Gonzalez-Diaz[2], H. Emling[2], P. Diaz Fernandez[4], L.M. Fraile[9], O. Ershova[2], H. Geissel[2,10], B. Jonson[11], H. Johansson[11], N. Kalantar-Nayestanaki[12], R. Krücken[13], T. Kröll[3], J. Kurcewicz[2], C. Langer[2], T.Le Bleis[12], Y. Leifels[2], G. Münzenberg[2], J. Marganiec[2], T. Nilsson[11], C. Nociforo[2], A. Najafi[12], V. Panin[2], S. Paschalis[3], R. Plag[2], R. Reifarth[2], V. Ricciardi[2], D. Rossi[2], H. Scheit[3], H. Simon[2], C. Scheidenberger[2,10], S. Typel[2], J. Taylor[7], Y. Togano[14], V. Volkov[3], H. Weick[2], A. Wagner[15], F. Wamers[2], M. Weigand[2], J.S. Winfield[2], D. Yakorev[15], and M. Zoric[2]

[1] *Saha Institute of Nuclear Physics, Kolkata 700064, India*
[2] *GSI Helmholtzzentrum fur Schwerionenforschung GmbH, D-64291 Darmstadt, Germany*
[3] *Technische Universitat Darmstadt, 64289 Darmstadt, Germany*
[4] *Universidade de Santiago de Compostela, 15706 Santiago de Compostela, Spain*
[5] *Instituto Tecnologico de Aeronautica, Sao jose dos Campus, Brazil*
[6] *University of Surrey, Guildford GU2 5XH, United Kingdom*
[7] *University of Liverpool, Liverpool L69 7ZE, United Kingdom*
[8] *INFN, LNL, Legnaro, Italy*
[9] *Universidad Complutense de Madrid, Avenida Complutense, E-28040 Madrid, Spain*
[10] *Physikalisches Institut, Giessen, Germany*
[11] *Fundamental Fysik, Chalmers Tekniska Hogskola, S-412 96 Goteborg, Sweden*
[12] *KVI-CART, The Groningen university, The Netherlands*
[13] *Physik Department E12, Technische Universität München, 85748 Garching, Germany*
[14] *The Institute of Physical and Chemical Research (RIKEN), Japan and*
[15] *Helmholtz-Zentrum Dresden-Rossendorf, D-01328 Dresden, Germany*

(Dated: May 25, 2016)

The first direct experimental evidence of multiparticle-hole ground state configuration of the neutron-rich ^{33}Mg isotope has been obtained via intermediate energy (400 A MeV) Coulomb dissociation measurement. It has been observed that the major part $\sim (70 \pm 13)\%$ of the cross-section has populated the excited states of ^{32}Mg after the Coulomb breakup of ^{33}Mg. The shapes of the differential Coulomb dissociation cross sections in coincidence with different core excited states favor that the valence neutron occupies both the $s_{1/2}$ and $p_{3/2}$ orbitals. These experimental findings suggest a significant reduction and merging of $sd-pf$ shell gaps at N $\sim$ 20 and 28. The ground state configuration of ^{33}Mg is predominantly a combination of ^{32}Mg(3.0,3.5 MeV;2^-,1^-)$\bigotimes \nu_{s_{1/2}}$, ^{32}Mg(2.5 MeV;2^+)$\bigotimes \nu_{p_{3/2}}$ and ^{32}Mg($0;0^+$)$\bigotimes \nu_{p_{3/2}}$ etc. . The experimentally obtained quantitative spectroscopic information for the valence neutron occupying the s and p orbitals, coupled with different core states are in agreement with MCSM calculation using 3 MeV as shell gap at N=20.

PACS numbers: 21.10;23.90.+w;25.6.-t;27.3.+t:

Recently, the observations of break down of traditional "magic numbers" [1] in the exotic nuclei far from beta-stability line are one of the key issues in the nuclear structure physics and significant efforts have been put on both the experimental investigations [2, 3, 5–12] and the theoretical studies [13–16]. The first observation of the disappearance of the magic number was reported by Thibault et al., [2] based on the mass measurements in the neutron rich ^{31,32}Na isotopes [2]. Later similar observation was reported, also in ^{33}Mg. [3]. The onset of deformations in the nuclei, ^{32}Mg [4], ^{31}Na [5], ^{30}Ne [7], with N=20 shell closure were also observed. These phenomena were proposed to originate due to substantial contributions from the "intruder" pf configurations over normal sd-shell in the ground state wave functions because of reducing or vanishing sd-pf shell gap (N = 20). The N=20 isotones for $Z \sim 10-12$ are considered to belong to the "island of inversion" [13]. The breakdown of the N=20 shell gap can be explained by the nucleon-nucleon interaction (strongly attractive monopole interaction of the tensor force) [14, 15]. Fortune [16] has shown that the measured data on reduced matrix element of the first excited 2^+ state of the ^{32}Mg [4] can be explained by a dominant sd-shell configuration in the ground state of this isotope.

Hence, it is important to study detailed shell configurations of the ground state of the neutron-rich nuclei with N=21 isotones. Many different experiments [3, 6, 8–12] have been performed to unravel the structure of ^{33}Mg(N=21) but until now neither the ground state parity nor the shell configuration was confirmed. From the measured negative sign of the magnetic moment , a pure 3p-2h ground state configuration and $3/2^-$ ground state spin and parity was suggested [10]. On the

* ushasi.dattapramanik@saha.ac.in

contrary, a $3/2^+$ ground state spin, parity with 4p-3h or 2p-1h configuration have been assigned through β-decay measurements i.e., ^{33}Mg to ^{33}Al [9] and ^{33}Na to ^{33}Mg [6]. Narrow longitudinal momentum distribution (150±3 MeV/c) of ^{32}Mg was observed by knockout reaction of this (S_n=2.23 MeV) nucleus [11]. The measured longitudinal momentum distribution was in good agreement with both ground state spin of $3/2^+$ or $3/2^-$, considering mixed configurations of ^{32}Mg in excited states coupled with a neutron in *sd-pf* shell [11, 12]. In this article, we report the first direct experimental evidence on multiparticle-hole ground state configuration of the neutron-rich ^{33}Mg isotope, and sufficient reduction as well as merging of the $sd-pf$, shell-gaps at N=20 and 28, obtained via the intermediate energy (400 A MeV) Coulomb dissociation measurements. This article reports detailed major components of the ground state configuration of this neutron-rich nucleus with an original view of the exotic structure.

The experiment (GSI: S306) was performed using the FRS-ALADIN-LAND setup, at GSI, Darmstadt. The radioactive beam, ^{33}Mg was produced by the fragmentation of the ^{40}Ar beam with energy 540 A MeV. After the separation by the FRS [22], the beam ($\sim$ 2 % of total cocktail beam at reaction target) was transported to the experimental site, where the complete kinematic measurements were performed using secondary ^{208}Pb, ^{12}C targets and empty target. The target was surrounded by 160 NaI detectors used for detecting the γ-rays from the excited nuclei. The γ-rays were reconstructed through add-back procedure among neighboring crystals of highest energy deposition followed by the Doppler correction. The γ-sum energy spectra was obtained by adding the coincident γ-rays. The detection efficiencies of the γ-rays under the experimental condition were estimated by GEANT simulation. The validation of simulated results has been performed by comparing the experimental data of standard calibrated γ-rays sources with the simulated one. The efficiency of the sum-energy spectra are in agreement within 10%. After the reaction at the secondary target, the reaction fragments as well as the unreacted beam were bent by a Large Dipole Magnet and ultimately detected at the time of flight wall detector. By the use of energy-loss and time of flight measurements, as well as position measurements in front and behind the dipole magnet, the nuclear charge, the velocity, the scattering angle, and the mass of the fragments has been determined. The emitted neutrons from the excited projectile were forward focused and tracked with the Large Area Neutron Detector [23]. For details of the set up, see [25–27].

The excitation energy E^* of the projectile, ^{33}Mg, prior to decay is obtained by reconstructing the invariant mass by measuring four momentum of all the decay products of the projectile after breakup [17–20]. The Coulomb dissociation (CD) cross section for the ^{208}Pb target (2.0 g/cm^2) has been determined after subtracting the nuclear contribution which was obtained from the data with a ^{12}C target (0.9 g/cm^2) with proper scaling factor (1.8) [24].

The experimental data on the electromagnetic excitation to non-resonant continuum has been analyzed using the direct breakup model to explore the ground state configuration [17–21]. When a projectile passes by a high Z target, it may be excited by absorbing the virtual photons from the time varying Coulomb field and the nucleus breaks up into a neutron and the core. This one neutron removal differential Coulomb dissociation cross section (CD) can be expressed as an incoherent sum of the components of $d\sigma_c^\pi/dE^*$ corresponding to the different core states with the spin and parity, populated after breakup. This can be expressed through the following equation [17]:

$$\frac{d\sigma_c^\pi}{dE^*} = \frac{16\pi^3}{9\hbar c} N_{E1}(E^*) \sum_j C^2S(I_c^\pi, nlj) \times \sum_m | < q|(Ze/A)rY_m^l|\psi_{nlj}(r) > |^2 \quad (1)$$

$N_{E1}(E^*)$ is the number of virtual photons as a function of the excitation energy E* [28]. $\psi_{nlj}(r)$ and $< q|$ represent the single-particle wave function of the valence neutron in the projectile ground state and the final state wave-function of the valence neutron in the continuum, respectively. The out going neutron wave function in the continuum is considered as a plane wave. $C^2S(I_c^\pi, nlj)$ represents the spectroscopic factor with respect to a particular core state I_c^π of the valence neutron in the projectile ground state.

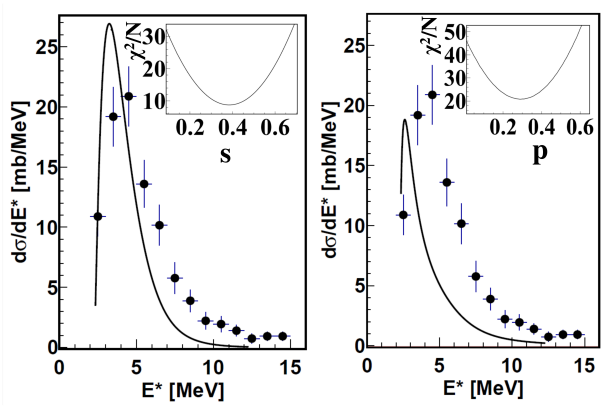

FIG. 1. Total inclusive differential CD cross section with respect to the excitation energy (E*) of ^{33}Mg. The smooth curve is the cross section on the basis of direct breakup model using a plane wave approximation for the s (left panel) and the p-orbital (right panel) neutron, respectively. Inset of the each panel of figure shows the χ^2/N for the fit between the experimental differential CD with that obtained from the direct breakup model calculation.

By comparing the experimental CD cross section with the calculated one, information on the ground state properties such as the orbital angular momentum of the valence nucleon and the corresponding

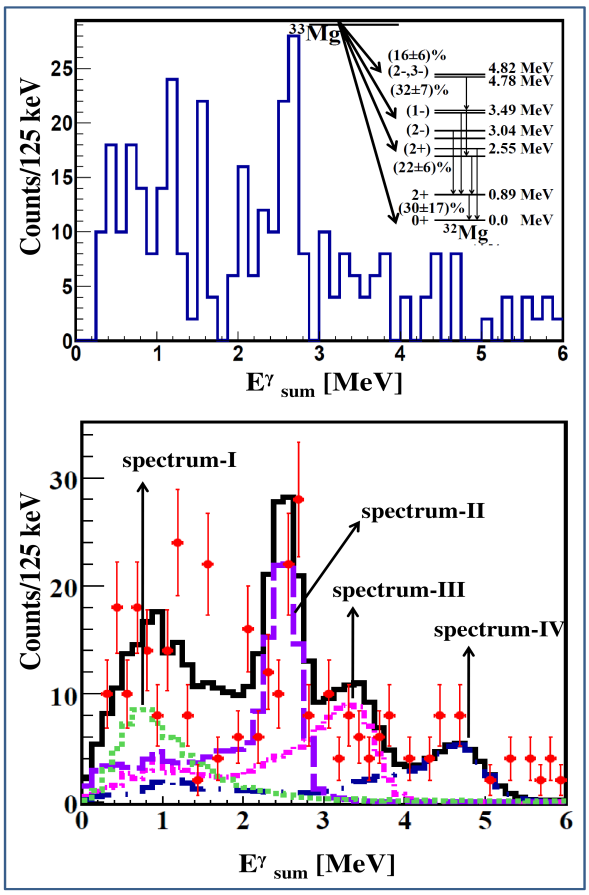

FIG. 2. (top)The observed sum-energy spectrum of γ-rays, transitions from the excited states of ^{32}Mg after Coulomb breakup of ^{33}Mg. The inset shows a partial scheme of levels in ^{32}Mg and population of those states after Coulomb breakup. (bottom) The solid black line represents addition of simulated sum-energy spectrum of γ-rays decaying from various core excited states and experimental atomic background. Experimental atomic background is represented by spectrum-I. Spectrum-II, spectrum-III, spectrum-IV are representing simulated sum-energy spectra of γ-rays decaying from 2.5 MeV excited state, combination of 3.5, 3.0 MeV states and 4.78, 4.82 MeV states, respectively.

spectroscopic factor may be obtained. The core state which is coupled with the neutron, can be identified by the characteristic γ-rays decaying from the core after the breakup. In order to compare with the experimental results, all the calculated results shown in this article are convoluted with the response function [19, 29].

The total Coulomb dissociation cross section for ^{33}Mg $\rightarrow$ ^{32}Mg + neutron amounts to 106±14 mb, integrated up to 9 MeV excitation energy. Figure 1 shows the total Coulomb dissociation cross-section for ^{33}Mg $\rightarrow$ ^{32}Mg + n. No resonance-like structure has been observed in the excitation spectra of ^{33}Mg [fig. 1]. The total inclusive experimental differential CD cross section has been fitted using the calculated one. The insets of the fig. 1[left] and fig. 1[right] show the χ^2/N for fitting with variation of the valence neutron spectroscopic factor in the s and p orbitals, respectively. The best fit suggests that the valence neutron coupled with ^{32}Mg (0^+) in the ground state only cannot explain the data.

Fig. 2 [top] shows sum-energy spectrum of the γ-rays decaying from the excited states of ^{32}Mg after Coulomb breakup of ^{33}Mg. This spectrum is obtained in coincidence with incoming beam, ^{33}Mg, the outgoing fragment, ^{32}Mg and one neutron. This spectrum reflects the ground state configuration of ^{33}Mg as the reaction mechanism demands [17]. The γ-rays spectra from the reactions at high energies on high-Z targets are strongly affected (up to energies of a few 3 MeV) by the low-energy background. The low-energy background originates from atomic interactions of the beam with the lead target [30]. The shape of the low-energy background was obtained from the γ-rays spectrum in coincidence with the noninteracting Mg beam (spectrum-I in fig.2 [bottom]). To understand the sum-energy spectra of the γ-rays, a detailed response corresponding to the detection sum-energy spectra of the γ-rays, decaying from a particular excited state in the experimental situation has been generated with the Monte Carlo code GEANT in a simulation procedure. The spectrum-II, spectrum-III and spectrum-IV in the fig. 2[bottom], are the simulated sum-energy spectra of γ-rays decaying from 2.5 MeV excited state, a combination of 3.5 and 3.0 MeV states and a combination of 4.78 MeV, 4.82 MeV states, respectively. In the simulation, decay scheme of various excited states of ^{32}Mg was considered as reported in the literature [33] and the partial level scheme of ^{32}Mg is shown in the inset of Fig. 2 [top]. The solid (black online) line in the fig. 2[bottom] represents the sum spectrum of spectrum-I, II, III and IV. The partial Coulomb breakup cross-sections of ^{33}Mg for populating various excited states of ^{32}Mg have been extracted from the invariant mass spectra in coincidence with the sum-energy of γ-rays spectra of above mentioned three different regions. The detection efficiency, feeding corrections from higher states of γ-ray have been obtained from detailed simulation. The detection efficiencies of the sum-energy of γ-rays from 2.3 MeV to 2.8 MeV, 2.9 MeV to 4.0 MeV, and 4.0 MeV to 5.7 MeV are 41±4%, 41±4% and 47±5%, respectively. Thus partial CD cross-sections for populating above three sets of excited states of ^{32}Mg are 23±5 mb, 34±6 mb and 17±6 mb. These cross-sections are obtained from the Pb-target data after subtracting its nuclear part. The same for ground state, is 32 ± 17 mb which is obtained from the difference between the total CD cross-section and the cross-sections of the excited states. The inset of figure 2[top] shows the relative population of different core excited states after Coulomb breakup. Thus the data analysis shows that the overwhelming part $\sim$ (70±13)% of the cross section leaves the core, ^{32}Mg in its excited states.

It is interesting to note that after the Coulomb breakup of ^{17}C, major part ($\sim$ 91 %) of the core, ^{16}C, was pop-

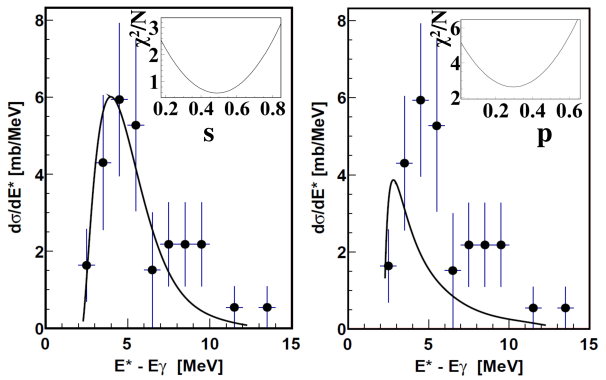

FIG. 3. Partial differential CD cross section of ^{33}Mg with respect to (E*-E$_\gamma$) in coincidence with ^{32}Mg in excited states $\sim$ 3.0,3.5 MeV (I$^\pi = 1^-, 2^-$). The smooth curve is the cross section on the basis of direct breakup model using plane wave approximation for the s-wave (left) and the p-wave (right) neutron, respectively. Inset of each panel of the figure shows the χ^2/N for the fit

ulated in excited states [17] and the ground state spin, parity and the single-particle configuration of ^{17}C, obtained from the Coulomb breakup analysis [17] was in agreement with the knockout reaction [31]. The present analysis of Coulomb breakup of ^{33}Mg has been performed in similar manner to that of ^{17}C [17].

The ground state spin of ^{33}Mg is 3/2 as suggested by two recent independent experiments [9, 10]. But the parity and the single-particle configuration is under debate. To explore further this issue, further data analysis has been performed. Fig. 3 shows the differential CD cross-section in coincidence with sum-energy γ-rays of $\sim$ 3.5 MeV, 3.0 MeV. The data has been fitted with the direct breakup model calculation. The insets of that figure 3-left and 3-right shows the variation of χ^2/N as a function of spectroscopic factor of the valence neutron, occupying the s and p orbitals, respectively. The χ^2/N for the fit (figure 3) clearly suggests that the valence neutron occupies the s orbital with the spectroscopic factor 0.47$\pm$0.08. Even for 4σ error (i.e, within 99.99 % confidence limit), the spectroscopic factor will be between 0.15 to 0.8. On the contrary, similar analysis in coincidence with sum-energy γ-rays of 2.5 MeV, can explain the data using the neutron, occupying either the s or p orbitals. Fig. 4 shows the differential CD cross-section in coincidence with γ-decay of energy $\sim$ 2.5 MeV. This can be understood as 2.5 MeV γ-rays can be obtained from de-excitation of the 3.5 MeV (1$^-$) state as well as the 2.55 MeV (2$^+$) state which are opposite parity states. Similarly as above, the spectroscopic factor of 0.26$\pm$0.07 can be obtained for the valence neutron occupying p orbital. coupled with ^{32}Mg(2.5 MeV;2$^+$). Unlike other two situations, the cross-section with large statistical error, the spectroscopic factor for this situation i.e., ^{32}Mg(0;0$^+$)$\bigotimes\nu_{p_{3/2}}$ is obtained from the ratio of the experimental cross-section with the calculated one.

Thus, different components of the ground state configuration of this nucleus are ^{32}Mg(3.0,3.5MeV;1$^-$, 2$^-$)$\bigotimes\nu_{s_{1/2}}$, ^{32}Mg(2.5MeV;2$^+$)$\bigotimes\nu_{p_{3/2}}$ and ^{32}Mg(0;0$^+$)$\bigotimes\nu_{p_{3/2}}$ etc. and it is suggested that the ground state parity is negative and the spin could be 3/2 which was proposed earlier [9, 10]. Considering this spin and parity, a tentative forth component of ground state conficuration as, ^{32}Mg(4.78, 4.82 MeV; 2$^-$)$\bigotimes\nu_{s_{1/2}}$ could be considered. Since the exclusive CD cross-section associated with this core state is small with large error, the spectroscopic factor can be obtained by ratio of the cross-section. It is interesting to note that both measurement of the magnetic moment [34] and the Coulomb breakup [27] of neutron-rich isotope, ^{34}Al(N=21) support multi-particle-hole ground state configuration. Fig. 5 shows the total experimental differential Coulomb breakup cross-section (black filled circles) of ^{33}Mg overlaying with the sum of the four exclusive calculated CD cross-sections for above mentioned four components of ground state configuration of ^{33}Mg. The mesh (red in online) shaded region is representing the associated error obtained from various contributions. The shaded region with closely spaced left tilted lines (pink in online), right tilted lines (black colour in online), wide spaced left tilted lines (green in online), and solid filled shaded region are presenting the calculated differential CD cross-section of ^{33}Mg with associated error for the components, ^{32}Mg(3.0,3.5MeV;1$^-$, 2$^-$)$\bigotimes\nu_{s_{1/2}}$, ^{32}Mg(2.5MeV;2$^+$)$\bigotimes\nu_{p_{3/2}}$, ^{32}Mg(4.8MeV;2$^-$)$\bigotimes\nu_{s_{1/2}}$, and ^{32}Mg(0;0$^+$)$\bigotimes\nu_{p_{3/2}}$, respectively. These errors are the errors associated with spectroscopic factors which are obtained via fitting between the experimental CD data in coincidence with respective core state(s) and the calculated ones, except, ground state core and core excited states at 4.78, 4.8 MeV. In these situations, the spectroscopic factors with errors are obtained through ratio of the calculated and experimental cross-sections.

Table 1. shows the partial experimental Coulomb dissociation cross sections of ^{33}Mg for different core states

TABLE I. Partial Coulomb dissociation cross sections of ^{33}Mg for different core states up to excitation energy (E$_c$+9.0) MeV . The corresponding spectroscopic factors from calculations [11] and the ones derived from the experiment are quoted.

Core state I^π (E_c MeV)		Neutron orbital	Cross section (mb)	Spectroscopic factor Shell model	Experiment
experiment [33]	calculated [11]			[11]	
0$^+$ (0.0)	0$^+$ (0.0)	$1p_{3/2}$	32 $\pm$ 17	0.12	0.19$\pm$0.1
2$^+$(2.5)		$1p_{3/2}$	23 $\pm$ 5		0.26$\pm$0.07
	2$^+$(3.01)			0.2	
2$^-$(3.0		$1s_{1/2}$			
1$^-$(3.49)		$1s_{1/2}$	34 $\pm$ 6		0.47$\pm$0.08
	1$^-$ (3.81)	$1s_{1/2}$		0.21	
	2$^-$ (3.94)	$1s_{1/2}$		0.27	

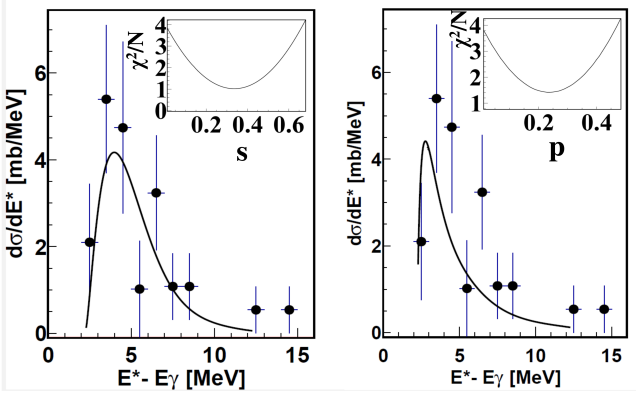

FIG. 4. Partial differential CD cross section of ^{33}Mg with respect to ($E^* - E_\gamma$), in coincidence with ^{32}Mg in excited state $\sim$ 2.5 MeV ($I^\pi = 2^+$). The smooth curve is the cross section on the basis of direct breakup model using plane wave approximation for s-wave (left-panel) and for p-wave (right-panel). Inset of each panel of figure shows the χ^2/N for the fit.

with the spectroscopic factor for valence neutron occupation. The corresponding spectroscopic factors from Monte Carlo shell model (MCSMmod) calculations with SDPF-M interaction [11, 32] are shown in the fifth column of table 1. The experimental results are in good agreement with the calculation. It is evident from table 1 that a large spectroscopic factor for the valence neutron (N=21) in the $s_{1/2}$ orbital is obtained. It was shown through shell model calculation that multiparticle-hole (np-nh) excitations across the shell-gap may lead to the deformation in this region [13]. The reaction data [8] support prolate deformation of this isotope. The occupation of the valence neutron (N=21) in $s_{1/2}$ orbital is possible with large deformation ($\beta_2 \sim$ 0.45-0.5) where the extruder 1/2[200] deformed Nilsson state with 60-70 % component of j=1/2 orbital is available near Fermi level [38].

It was shown by Ripka and Larry [35] that the measured magnetic moments in odd-A nuclei of this mass region deviate from the Schmidt values. But those experimental values could be explained by a calculation using an odd nucleon coupled with a deformed Hartree-Fock core [35]. Similarly, a valence neutron occupying a 1/2[200] deformed Nilsson orbital can explain recent measured magnetic moments of ^{33}Mg [10]. It is shown that magnetic moment calculated by a particle plus rotor with deformation 0.45 for 1/2[200] state is -0.86 μ_N [36] and this value is in agreement with measured value of -0.7456(5) μ_N [10]. With this deformation, both 1/2[330] and 3/2[321], deformed intruder Nilsson states with component of $p_{3/2}$ orbital are available near the Fermi level. And indeed, an experimental signature for the occupation of the p orbital by the valence neutron has been observed in the present experiment.

The present experimental data analysis concludes that the ground state of ^{33}Mg, predominantly consists of deformed multi-particle-hole core of ^{32}Mg coupled with a valence neutron(s) in the deformed Nilsson 1/2[200] and 3/2[321] states, etc. The deformation of ^{33}Mg plays key role in the exotic nuclear structure [37–39]. It is interesting to note that even ^{33}Mg (sn=2.3 MeV) is much loosely bound than ^{25}Ne (Sn=4.2 MeV), but spatial extension of valence neutron of ^{33}Mg is less or equal of that of ^{25}Ne. This inhibition of spatial extension of the loosely bound valence neutron can be explained as co-relations between valence neutrons and those due to static or dynamic deformation of the core [39]. Thus ^{33}Mg can be considered as an unique example of deformed, multi-quasi-particle, loosely bound nucleus. In the present scenario, the states consist mainly of low-l orbital components at high deformation in the loosely-bound nuclei [37]. The occupation of the valence neutron in 1/2[200] state can be responsible for the structure of ^{33}Mg which is completely decoupled from the rest of the system i.e., ^{32}Mg. The deformation in this nucleus can be determined by the intrinsic structure of the weakly bound neutron orbital, or the shape of the core or interplay of both. Thus a rich variety of shape co-existence phenomena or structure are expected to be observed. The shape of the spatial distribution of ^{33}Mg may be different than that of core, ^{32}Mg. A detailed experimental and theoretical investigation of this nucleus may provide important information about the exotic structure of deformed, multi-quasi-particle nucleus.

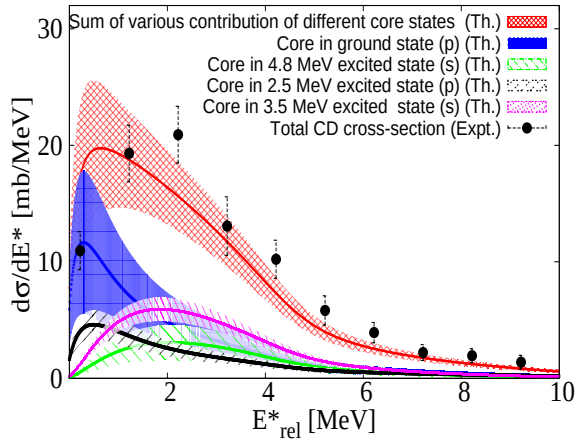

FIG. 5. Total experimental (black filled circle data) differential CD cross- section of ^{33}Mg is overlaid with the sum of various components of calculated CD cross-sections (red colour solid line), which populate various core, ^{32}Mg, excited states. The (red online) mesh shaded region is the error obtained from various contributions through error propagation. The shaded region filled with right tilted lines (black colour in online), closely spaced left tilted lines (pink in online), left tilted lines (green in online) and solid filled are presenting the errors associated with calculated CD cross-sections for various exclusive ground state components of ^{33}Mg and the errors are obtained from those associated with spectroscopic factors of valence neutron(s), occupying $p_{3/2}$, $s_{1/2}$, $s_{1/2}$ and $p_{3/2}$ orbitals coupled with core in 2.5 MeV, 3.5 MeV, 4.8 excited and ground states, respectively. See text for details.

In conclusion, the present experimental data of the Coulomb dissociation of ^{33}Mg(N=21) provides first evidence of multi-particle-hole ground state configuration and the valence neutron(s) is occupying the s and the p orbitals. These observations confirm significant reduction and merging of shell gaps, at N=20 and 28 for this neutron-rich nucleus. The valence neutron of this isotope occupies partially the $s_{1/2}$ orbital, which is an indirect evidence of large deformation (β $\sim$0.45) because the extruder 1/2[200] is only available near Fermi level for N=21. Thus, through the electric dipole response from the ground state to the continuum, a large deformation as well as multiparticle hole ground state configurations can be obtained for ^{33}Mg. It will be interesting to study exotic shape evolution of the neutron-rich nuclei near traditional "magic numbers" using future facilities like FAIR, FRIB or Hi-ISOLDE etc.

[1] M. Geoppert Mayer, Phys. Rev.**75**, 1969 (1949). O. Haxel, Phys. Rev.**75**, 1766 (1949).

[2] C. Thibault *et al.*, Phys. Rev. C **12**, 644 (1975).

[3] N.A. Orr *et al.*, Phys. Lett. B **258**, 84 (1991). X.G. Zhou *et al.*, Phys. Lett. B **260**, 285 (1991).

[4] T. Motobayashi *et al.*, Phys. Lett. B **346**, 9 (1995).

[5] B.V. Pritychenko *et al.*, Phys. Rev. C **63**, 011305(R) (2000).

[6] S. Nummela *et al.*, Phys. Rev. C **64**, 054313 (2001).

[7] Y. Yanagisawa *et al.*, Phys. Lett. B **566**, 84 (2003).

[8] Z. Elekes *et al.*, Phy. Rev. C **73**, 044314 (2006).

[9] V. Tripathi *et al.*, Phys. Rev. Lett. **101**, 142504 (2008).

[10] D.T. Yordanov *et al.*,et al., Phys. Rev. Lett. **99**, 212501 (2007).

[11] R. Kanungo *et al.*, Phys. Lett. B **685**, 253 (2010).

[12] Gerda Neyens, Phys. Rev. C **84**, 064310 (2011).

[13] E. K. Warburton, J.A. Becker, B.A. Brown, Phys. Rev. C **41**, 1147 (1990).

[14] A.De. Shalit *et al.*, Phys. Rev. **92**, 1211 (1953).

[15] T. Otsuka *et al.*, Phys. Rev. Lett. **104**, 012501 (2010).

[16] H.T. Fortune, Phys. Rev. C **85**, 014315 (2012).

[17] U. Datta Pramanik *et al.*, Phys. Lett. B **551**, 63 (2003).

[18] R. Palit, et al., Phys. Rev.C.**68**, 034318 (2003)

[19] C. Nociforo *et al.*, Phys. Lett. B **605**, 79 (2005).

[20] U. Datta Pramanik, Prog. in Particle and Nucl. Phys. **59**, 183 (2007).

[21] T. Aumann and T. Nakamura, Phys. Scr.T152. 014012 (1999).

[22] H. Geissel *et al.*, Nucl. Instrum. Methods B **70**, 286 (1992).

[23] T. Blaich *et al.*, Nucl. Instrum. Methods A **314**, 136 (1992).

[24] C. J. Benesh, B.C. Cook, J.P. Vary, Phys. Rev. C **40**, 1198 (1989).

[25] C. Caeser *et al.*, Phys. Rev. C **84**, 064310 (2013).

[26] A. Rahaman *et al.*, EPJ web **66**, 02087 (2014).

[27] S. Chakraborty *et al.*, EPJ web **66**, 02019 (2014).

[28] C.A. Bertulani and G.Baur, Physics Reports **163**, 299 (1988).

[29] K. Boretzky *et al.*, Phys. Rev. C **68**, 024317 (2003).

[30] R.Anholt *et al.*, Phys. Rev. A **33**, 2270 (1986).

[31] V. Maddalena *et al.*, Phys. Rev. C **63**, 024613 (2001).

[32] Y. Utsuno, T. Otsuka, T. Mizusaki, M.Honma, Phys. Rev. C **64**, 011301R (2001).

[33] http://www.nndc.bnl.gov

[34] P. Himpe *et al.*, Phys. Lett. B **658**, 203 (2008).

[35] G. Ripka and L.Zamick Phys. Lett. **23**, 347 (1966).

[36] D.T. Yordanov *et al.*, Phys. Rev. Lett. **104**, 129201 (2010).

[37] T. Misu, W. Nazarewicz, and A. Aberg, Nucl. Phys. A**614**, 44 (1997)

[38] Ikuko Hamamoto, Phys. Rev. C **69**, 041306 (2004).

[39] F.M. Nunes Nucl. Phys. A**757**, 349 (2005)